Available online at www.sciencedirect.com

SciVerse ScienceDirect

Energy Procedia 37 (2013) 3413 – 3423

Energy Procedia

GHGT-11

Simulation of the near field physiochemical impact of CO_2 leakage into shallow water in the North Sea

Marius Dewar*, Wei Wei, David McNeil, Baixin Chen,

School of Engineering Physics Science, Heriot-Watt University, Edinburgh, EH14 4AS, United Kingdom

Abstract

This study involves developing a small scale two-fluid numerical model to simulate CO_2 bubble leakage from potential storage sites, and to predict the plume dynamics and dissolution of the bubbles dispersed from the sediments into the water column and beyond with the resultant seawater pH change. Calibrating results to lab and in-situ experimental data, the model is applied for simulations of potential sub-seabed reservoir leakages in locations within the North Sea's shallow waters where carbon storage is being considered. The model consists of a sub-model that predicts the initial bubble size forming on the water basin and further sub models for mass and momentum exchange to the seawater. It is found that it is unlikely that bubbles smaller than 30mm diameter will reach the water surface and atmosphere when leaked from depths greater than 20m, and will fully dissolve in the waters creating pH changes of various concentrations dependent on the plume dynamics and ocean currents at the leakage sites.

© 2013 The Authors. Published by Elsevier Ltd.
Selection and/or peer-review under responsibility of GHGT

Keywords, CO_2; Bubble; Dissolution; Numerical Model; Carbon Capture and Storage; CCS;

1. Introduction

Carbon Capture and Storage (CCS) is considered to be a crucial step in mitigating the effects of climate change caused by greenhouse gases within the atmosphere. Sub-seabed, offshore storage is of particular interest due to the reduced risk to human life in the case of leakage from the reservoir in comparison to that of onshore storage [1]. Projects have been operating within the North Sea including those by Gaz de France Production Netherland B.V. (GPN) in the K12-B project [2] and by Statoil in the Sleipner west gas field [3], both separating the high content of CO_2 from the natural gas supplied from the reservoir and re-

* Corresponding author. Tel.: +44 131 451 3779; fax: +44 131 451 3129.
E-mail address: md61@hw.ac.uk.

1876-6102 © 2013 The Authors. Published by Elsevier Ltd.
Selection and/or peer-review under responsibility of GHGT
doi:10.1016/j.egypro.2013.06.230

injecting it into the geological formations below the seabed [3].

A major concern with CCS is the risk and timeline for safe and efficient storage, with the likelihood of leakage from the reservoir and the effect this would have on marine life and the environment [3], where leakages can occur from faults in sediment rock to wellbore ruptures. Although these risks are considered be less than that of the equivalent leakage of hydrocarbons, a rapid source of CO_2 can potentially cause an instant danger to human life at concentrations above only 7% volume (mixed in air) [4]. A detailed analysis is therefore required investigating the hazards caused from sub-seabed CCS leakage and the effects on the environment within the local waters [3, 5], investigated through the dissolution mechanism, dynamics of the leakage plume, interactions between the seawater and the dissolved CO_2 solution including the pH change of the waters [6, 7], and finally the possibility of CO_2 gas reaching the atmosphere.

The physiochemical impact from the CO_2 dissolution can be investigated through a number of mechanisms. Laboratory [8-11] and in-situ [5] experiments along with natural seepage investigations [12-14] provide vital data on the CO_2 dissolution rates through mass transfer and the dynamic movements of both the CO_2 and the dissolved CO_2 solution through momentum exchange. However full scale laboratory experiments are not feasible due to the size and costs involved, where political pressures limit the in-situ experiments [5]. Therefore numerical simulations are required to complete the gaps, using observational data and fluid properties from experiments to validate the model.

The objective of this study is to predict the effect that a leak would have on the local marine environment. The small scale movements of the CO_2 bubble plume will be modeled using a two phase numerical simulation, taking site properties to tune the model to the North Sea. Preliminary case studies may then be run to predict effects and chemical changes of the waters. Calibrating both in-situ and lab results with the simulations will allow the verification and validation of the model, approving its use for future simulations in shallow depth locations where CCS is being considered [3, 4].

2. Model for the dynamics of two phase flow

As the CO_2 plume leaks from the sediments it rises or falls due to buoyancy dependent on the density controlled by pressure and temperature [4]. This formation has been investigated in terms of deep droplet plumes through numerical modeling [15-19], however less research has been conducted on shallow water leakage where a rising plume of bubbles forms (less than 180m [4]) , with only a couple of recent models available [20, 21]. As the plume of bubble rises, dissolution occurs from mass transfer and momentum transfers to the seawater through drag forces. Solving the continuity and Navier-Stokes equations allows the two phase plumes to be simulated.

2.1. Governing equations for CO_2 and seawater plumes

The CO_2 bubble plume is referred to as the dispersed phase (subscript *d*), and the seawater carrier phase (subscript *c*), with the void fraction α calculated as:

$$\alpha_c + \alpha_d = 1$$

The large eddy simulation based governing equations for the seawater carrier phase are defined as:

$$\frac{\partial \overline{\rho}}{\partial t} + \frac{\partial \overline{\rho} u_i}{\partial x_i} = \dot{w}_{co_2} \tag{1}$$

$$\frac{\partial \overline{\rho} u_i}{\partial t} + \frac{\partial \overline{\rho} u_i u_j}{x_j} = -\frac{\partial \hat{p}}{\partial y} + \frac{\partial D_{ij}}{\partial x_i} + (\overline{\rho} - \rho_0) g + \dot{F} \tag{2}$$

$$\frac{\partial \overline{\rho} \hat{\phi}_k}{\partial t} + \frac{\partial \overline{\rho} \hat{\phi}_k u_j}{\partial x_j} = \frac{\partial}{\partial x_j}(\overline{\rho} D_k \frac{\partial \hat{\phi}_k}{\partial x_j}) + \frac{\partial \overline{\rho} \hat{q}_k}{\partial x_j} + \dot{w}_{co_2} \tag{3}$$

and the governing equations for the dispersed bubbles phase as:

$$\frac{\partial \hat{n}_d}{\partial t} + \frac{\partial \hat{n}_d u_{di}}{\partial x_i} = \hat{q}_{dn} \tag{4}$$

$$\frac{\partial \hat{\alpha}}{\partial t} + \frac{\partial \hat{\alpha} u_{dj}}{\partial x_j} = \hat{q}_{dco_2} - \frac{\dot{w}_{co_2}}{\rho_d} \tag{5}$$

$$\frac{\partial \overline{\rho}_d u_{dj}}{\partial t} + \frac{\partial \overline{\rho}_d u_{di} u_{dj}}{\partial x_j} = \hat{\alpha}(\overline{\rho}_d - \rho_w) g - \dot{F} \tag{6}$$

where $\overline{\rho}$ is the bulk density, (kg/m^3), u is the velocity (m/s), t is the time (s), x is the distance (m), $\dot{w}$ is the mass exchange rate (kg/m^3·s), p as the hydrostatic pressure (Pa), D is the dissipation term (kg/m·s^2), ρ_0 in the initial density (kg/m^3), g is gravity (m/s^2), $\dot{F}$ is the momentum exchange rate (kg/m^2·s^2), $\hat{\phi}$ is a scalar (temperature, salinity or CO_2 concentration), D_k is a diffusivity term (m^2/s), and $\hat{n}$ is the number density (m^{-3}) with a source term $\hat{q}$. The subscripts 'd', '*n*', '*w*', '*CO*$_2$' represent the dispersed phase, the number of bubbles, seawater and CO_2 respectively, with directional vectors represented though the subscripts '*i', 'j', 'k'*.

The modeling of turbulent transportation of water and CO_2 including the dissipation, diffusivities, have been formulated based on large eddy simulation [7, 16, 17]. The density of the seawater is calculated by using the international equation of state [22], with the density of CO_2 at depth calculated from Chemical handbook [23] and the pH changes are modeled by reverse engineering a model for calculating CO_2 concentrations from pH by Someya et al. [24].

2.2. Source terms for mass and momentum exchange terms

In order to solve the governing equations, sub-models for the mass and momentum exchange terms are required:

$$\dot{w}_{co_2} = \frac{3.0}{2.0}\left(\frac{\pi}{6.0}\right)^{1/3} \hat{\alpha}^{2/3} \hat{n}^{1/3} \frac{\pi}{d_{eq}} ShD_f (C - C_0) \tag{7}$$

$$\dot{F} = 0.75\left(\frac{\pi}{6.0}\right)^{1/3} \rho_d \hat{\alpha}^{2/3} \hat{n}^{1/3} C_d \left|u_j - u_{dj}\right| \left(u_j - u_{dj}\right) \tag{8}$$

Eq. (7) is the mass exchange from CO_2 dissolution, where d_{eq} is the equivalent diameter of the CO_2 bubble (m), Sh is the Sherwood number to calculate the effective mass transfer coefficient, D_f is the CO_2 diffusivity (m^2/s), C is the bubble surface CO_2 concentration (kg/m^3) and C_0 is the seawater CO_2 concentration (kg/m^3). Eq. (8) is the momentum exchange term through the drag force between the bubble and the seawater, where C_d is the drag coefficient.

3. Sub-model for the source terms

3.1. Drag coefficient for momentum – Bubbles

For the drag force in Eq. (8), the drag coefficient is required to describe how the drag changes with seawater at given size and shape of the bubbles. A correlation is proposed based on experimental data from Bigalke et al., [8, 9], converted from velocity and diameter data to that of Reynolds number and drag coefficient using Clift's equation for terminal velocity [25].

$$C_d = \frac{24}{\mathrm{Re}} f(\mathrm{Re}) \tag{9}$$

and the friction factor $f(\mathrm{Re})$ for bubbles is found to be:

$$f(\mathrm{Re}) = 1 + 0.045\,\mathrm{Re} - 1.50\times10^{-4}\,\mathrm{Re}^2 + 3.20\times10^{-7}\,\mathrm{Re}^3$$

where $\mathrm{Re} = \mathrm{d_{eq}\,u}/\nu$ is the Reynolds number, with ν as kinematic viscosity (m^2/s). This proposed sub-model is compared to a previous sub-model from Bozzano and Dent [26] as shown in Fig 1 (a) and Eq. (10).

$$C_d = f\left(\frac{a}{R_0}\right)^2 \tag{10}$$

where the friction factor f is found to be:

$$f = \frac{48}{\mathrm{Re}}\left(\frac{1+12M^{1/3}}{1+36M^{1/3}}\right) + 0.9\,\frac{Eo^{3/2}}{1.4\left(1+30M^{1/6}+Eo^{3/2}\right)}$$

and the deformation factor $(a/R_0)^2$ is found to be:

$$\left(\frac{a}{R_0}\right)^2 = \frac{10\left(1+1.3M^{1/6}\right)+3.1Eo}{10\left(1+1.3M^{1/6}\right)}$$

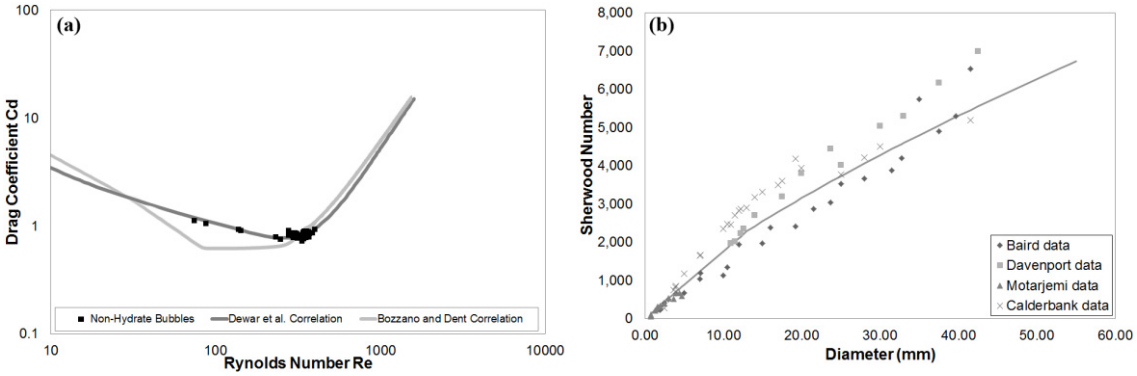

Fig. 1 (a) The drag coefficient correlation based on experimental data from Bigalke et al [8, 9] compared with that of Bozzano and Dent [26]; (b) The Sherwood number correlation matching experimental data collected by Zheng and Yapa [27].

3.2. Sherwood number for bubble mass transfer

For the mass exchange through dissolution, the effective mass transfer coefficient, k (m/s), is estimated by using a correlation of a Sherwood number, Sh, a ratio of convective to diffusive exchange, by which, how the shape, size and flow will affect the dissolution rate is simulated.

$$Sh = \frac{d_{eq}}{D_f} \cdot k \tag{11}$$

where the mass transfer coefficient will vary dependent on the bubble diameter and velocity [25]:

$$k = f_k(d_{eq}, u_d) \cdot D_f^{0.5}$$

and $f_k(d_{eq}, u_d)$ is the bubble size dependent correlation:

$$f_k(d_{eq}, u_d) = \begin{cases} 1.13\left(\dfrac{u_d}{0.45 + 20 d_{eq}}\right)^{0.5} & d_{eq} < 5mm \\ 6.5 & 5mm < d_{eq} < 13mm \\ \dfrac{0.219462}{d_{eq}^{0.25}} & d_{eq} > 13mm \end{cases}$$

Experimental data is collected by Zeng and Yapa [27] for the mass transfer coefficient k (m/s), rearranged to SI units in terms of Sherwood number in Fig 1 (b).

3.3. Initial bubble size

With buoyancy and drag being the major forces controlling dynamics [16], the size of the bubbles controls the movements, but also the dissolution rate. At given leakage rate, the smaller bubbles (with larger numbers of bubbles) the faster the dissolution can be because of the large surface area overall, whereas large bubbles rise further due to buoyancy.

To predict the size of a bubble forming on the sediment surface, a force balance is used, where the buoyancy and drag forces act against the surface and interfacial tension σ (N/m) holding the bubble to the sediments [28] through the sub-model:

$$\left[\left(\rho_w - \rho_{CO_2}\right) g \frac{{d_{eq}}^3}{6}\right]^2 + \left[\frac{C_d}{8}\rho_w u^2 {d_{eq}}^2\right]^2 = \left[d_{ch}\sigma\right]^2 \tag{12}$$

With surface and interfacial tension data from Espinoza et al. [29], and the channel diameter d_{ch} (m) estimated from sediment samples. A range of initial bubble sizes can be found dependent on the current and the changes in the sediment channels across the seabed.

This sub-model is an indication for low CO_2 leakage rates by using the original sediment channel size. As the flow increases, sediment particles become dislodged and taken up with the bubble plume through momentum [29] providing larger channels and in turn larger bubbles forming. In this case, a good estimation of d_{ch} is required.

4. Case Studies

4.1. In-situ properties and data

The site for a potential sub-seabed reservoir leakage is located in the coastal waters of the North Sea, looking at shallow depths of between 12 and 20 meters. To simulate the site within the model, fluid properties and location specific data are required. The salinity and temperature profiles of the seawater for summer and winter are taken from seasonal recordings within the North Sea [30], the average seawater bottom current are predicted based on a circulation model [31] and the leakage rate is determined through the higher estimates and predictions based on seepage rates from the Rangely enhanced oil recovery site [32].

4.2. Leakage scenarios

The case studies investigated in this study, with the parameters listed in Table 1, will show how seasonal data affects the dynamics and dissolution from summer to winter, along with the effect of the leakage depth, tidal currents, initial bubble sizes and the leakage rate.

For each case, the CO_2 bubbles are considered to leak from sediments with the channel size randomly distributed across the leakage area, from which the initial bubble size is calculated by Eq. (12). The final case study is an individual bubble model to determine the maximum bubble size at 20 meters depth that can fully dissolve before reaching the atmosphere

Table 1. The leakage scenario case studies

Case study	Depth	Season	Tidal current	Maximum initial bubble diameter	Leakage rate	Leakage area
1 - Summer season	20 m	Summer	5 cm/s	6.33 mm	0.1207 kg/s	15m × 15m
2 - Winter season	20 m	Winter	5 cm/s	6.33 mm	0.1207 kg/s	15m × 15m
3 - Reduced depth	12 m	Summer	5 cm/s	6.33 mm	0.1207 kg/s	15m × 15m
4 - No tidal current	20 m	Summer	0 cm/s	6.33 mm	0.1207 kg/s	15m × 15m
5 - Reduced diameter	20 m	Summer	5 cm/s	5.02 mm	0.1207 kg/s	15m × 15m
6 - Reduced leakage rate	20 m	Summer	5 cm/s	6.33 mm	0.05 kg/s	15m × 15m
7 - Largest diameter*	20 m	Summer	5 cm/s	30.00 mm	N/A	N/A

*case based on an individual bubble model to determine maximum bubble size that will dissolve in the waters

5. Model results and discussion

The model is designed to simulate both extreme and prolonged leaks to predict CO_2 and pH changes with time within the water column. This will provide data on how high the CO_2 bubbles rise in the water column, along with the pH changes showing where the greatest effect to marine life can be found.

5.1. Bubbles

The bubbles rise to their terminal height within the first 2.5 minutes showing that the bubbles have a fast rise velocity, but also a quick dissolution rate as seen in Fig 2, where the bubble reduces in diameter due to dissolution within a relatively small height from seabed.

Model results of selected key parameters describing CO_2 bubble plume characteristics are listed in Table 2. The seasonal changes from reducing the temperature will increase the buoyancy force, producing smaller initial bubbles and therefore reducing the rise height of the bubble plume. Reducing the depth also reduces the average bubble diameter, with the more buoyant bubbles breaking off the sediments at a faster rate; however as at this depth the bubbles also rise at a faster rate, the plume height is only marginally affected. Removing the tidal current effects increases the average bubble size and rise height due to the lack of drag force on the bubbles forming from the sediments. A reduced initial bubble diameter has the effect of reducing the buoyancy force therefore providing a lower terminal height for the bubble plume as shown in Fig 2 (b). Finally reducing the leakage rate has a slight increase in the average bubble size but a reduced bubble plume height from a more even spread of the mass.

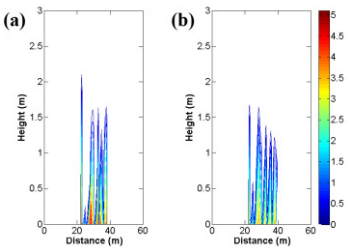

Fig 2. Simulated bubble plume 30 minutes from leak commencing; (a) summer season prediction; (b) reduced diameter (< 5mm)

Table 2. Model findings 30 minutes after leak commencing

Case study	Average initial diameter	Bubble plume rise height	Bubble plume height as % of depth	Maximum ΔpH
1 - Summer season	5.11 mm	2.37 m	11.84%	-2.04
2 - Winter season	5.09 mm	2.19 m	10.96%	-2.22
3 - Reduced depth	5.07 mm	2.28 m	19.03%	-2.08
4 - No tidal current	6.08 mm	2.85 m	14.25%	-1.63
5 - Reduced diameter	3.97 mm	1.65 m	8.27%	-2.29
6 - Reduced leakage rate	5.13 mm	1.97 m	9.85%	-1.83
7 - Largest diameter	30.00 mm	19.20 m	96.00%	N/A

5.2. pH change from dissolved CO_2 solution

The change in pH caused by an increase in acidity from carbonic acid forming is used to describe the effect on the marine environment from the CO_2 solution. As can be seen in Fig 3, the largest pH change is located towards the base of the plume due to the increase in density of this solution causing it to drop back to the sea floor.

As can be seen in Table 2 for maximum pH changes and Fig 4 for the volume of pH changes above 0.5 units, the reduced temperatures in winter provide an increase in maximum pH change. This is due to the bubble plume dissolving within a smaller distance providing larger volumes of large pH change. Reducing the depth also increases the maximum pH change slightly and increases the volume of large pH changes. Removing the tidal current has a large effect due to the larger bubbles and solution dispersing vertically giving a reduced pH change, but large volumes of pH changes are due to the lack of horizontal dispersion from the current. Reducing the bubble diameter gives dissolution within a smaller height so generates a larger maximum pH change and larger volumes of water with pH changes, but smaller volumes of acidity overall as shown in Fig 3 (b). Reducing the leakage rate has the effect of decrease in maximum pH and water volumes of pH change as there is less CO_2 to dissolve within the same volume.

6. Conclusions

In this study multiple scenarios of CO_2 leakage from low depth leakage sites have been modeled to simulate the effects of a CCS leakage within the North Sea's shallow waters. Matching results to lab and in-situ experimental data should verify and validate the sub-models use for simulations for CCS in the planning stages and leakage analysis.

The largest dangers are where large bubbles rise beyond the water surface (>3cm at depths shallower than 20 m) or many smaller bubble dissolve quickly giving a large pH change of the water, of which may further disperse into the sediments because of the negative buoyancy. This is one of the big concerns with the impact on sediment marine organisms. It must however be noted that this pH change is restricted within the area near the leakage sites and would dissipate quickly with the currents reducing the effect in the larger scales.

This model has been developed using experimental data to provide an indication of the effects that a CO_2 leak would have on the waters, however further lab and in-situ experimental results are required to determine the true value in predicating the effects of a leak on the environment.

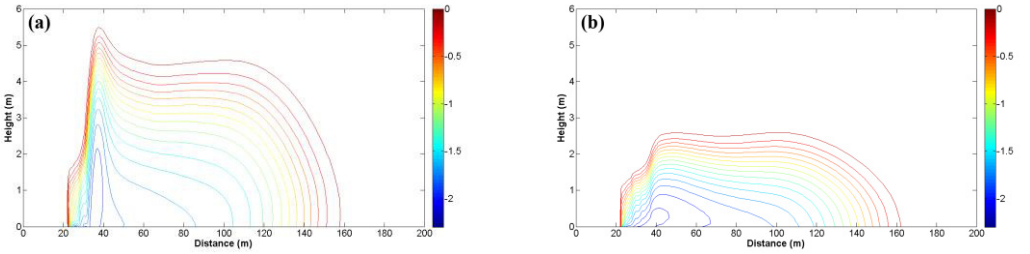

Fig 3. Simulated change in pH plume 30 minutes from leak commencing; (a) summer season prediction; (b) reduced diameter (< 5mm)

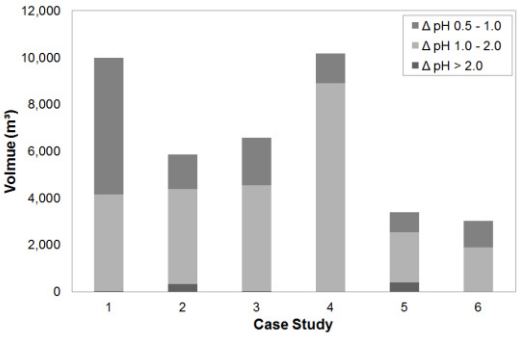

Fig 4. The volume of pH change within the waters for each case study after 30 minutes of leakage, e.g. for case study 2 there is 330m^3 of pH changes above 2, ~ 4,400m^3 of pH changes above 1 and ~ 5900m^3 of pH changes above 0.5.

Acknowledgements

This research as supported by the Natural Environment Research Council under grant NE/H013970, the FP7 Cooperation Work Program under grant 265847-FP7-OCEAN, and Research Council of Norway.

References

[1] Holloway, S. *Underground sequestration of carbon dioxide—a viable greenhouse gas mitigation option.* Energy, 2005. 30: 2318–2333.

[2] Van der Meer, L.G.H., Kreft, E., Gell, C., Hartman, J. *K12-B a test site for CO_2 storage and enhanced gas recovery*. SPE Europe/EAGE Annual Conference, 13-16 June 2005, Madrid, Paper SPE94128.

[3] IEA Greenhouse Gas R&D Programme (IEA GHG). *Assessment of Sub Sea Ecosystem Impacts*, 2008/8, August 2008.

[4] IPCC. *IPCC Special Report on Carbon Dioxide Capture and Storage*. Prepared by Working Group III of the Intergovernmental Panel on Climate Change [Metz, B., O. Davidson, H. C. de Coninck, M. Loos, and L. A. Meyer (eds.)], 2005, Cambridge University Press, Cambridge, United Kingdom and New York, NY, USA, 442 pp.

[5] Brewer, P. G., Chen, B., Warzinki, R., Baggeroer, A., Peltzer, E. T., Dunk, R. M. and Walz, P. *Three-dimensional acoustic monitoring and modeling of a deep-sea CO_2 droplet cloud*, Geophys. Res. Lett., 2006, 33(23), L23607.

[6] Blackford, J. C., N. Jones, R. Proctor, and J. Holt. *Regional scale impacts of distinct CO_2 additions in the North Sea*, Mar. Pollut. Bull., 2008, 56, 1461-1468, doi:10.1016/j.marpolbul.2008.04.048.

[7] Chen, B., Song Y., Nishio M. and Akai M. *Large-eddy simulation of double cloud formation induced by CO_2 dissolution in the ocean*, Tellus Series B, 2003, 55: 723– 730.

[8] Bigalke, N. K., Enstad, L. I., Rehder, G. and Alendal, G. *Terminal velocities of pure and hydrate coated CO_2 droplets and CH_4 bubbles rising in a simulated oceanic environment*, Deep-Sea Research Part I-Oceanographic Research Papers, 2010, 57(9), 1102-1110

[9] Bigalke, N. K., Rehder, G. and Gust, G. *Experimental Investigation of the Rising Behavior of CO_2 Droplets in Seawater under Hydrate-Forming Conditions, Environmental Science & Technology*, 2008, 42(14), 5241-5246.

[10] Ozaki, M., Minamiura, J., Kitajima, Y., Mizokami, S., Takeuchi, K. and Hatakenaka, K. *CO_2 ocean sequestration by moving ships*, Journal of Marine Science and Technology, 2001, 6(2), 51-58.

[11] Zheng, L. and Yapa, P. D. *Modeling gas dissolution in deepwater oil/gas spills*, Journal of Marine Systems, 2002, 31(4), 299-309.

[12] Caudron, C., A. Mazot, and A. Bernard. *Carbon dioxide dynamics in Kelud volcanic lake*, J. Geophys. Res., 2012, 117, B05102, doi:10.1029/2011JB008806.

[13] Esposito, A., G. Giordano, and M. Anzidei., *The 2002-2003 submarine gas eruption at Panarea volcano (Aeolian Islands, Italy): Volcanology of the seafloor and implications for the hazard scenario*, Mar. Geol., 2006, 227, 119-134, doi:10.1016/j.margeo.2005.11.007

[14] McGinnis, D. F., M. Schmidt, T. DelSontro, S. Themann, L. Rovelli, A. Reitz, and P. Linke. D*iscovery of a natural CO_2 seep in the German North Sea: Implications for shallow dissolved gas and seep detection,* J. Geophys. Res., 2011, 116, C03013, doi:10.1029/2010JC006557

[15] Alendal, G. and Drange H. *Two-phase, near-field modeling of purposefully released CO2 in the ocean*, J. Geophys. Res. 2001. 106, 1085–818 1096.

[16] Chen, B. Nishio M., Song Y. and Akai M. *The fate of CO_2 bubble leaked from seabed.* Energy Procedia, 2009. Vol. 1. Issue: 1. pp. 4969-4976

[17] Chen, B., Song Y., Nishio M, Someya S. and Akai M.. *Modelling near-field dispersion from direct injection of carbon dioxide into the ocean,* J. Geophys. Res. 2005, 110, C09S15, doi:10.1029/2004JC002567.

[18] Sato, T. and Hama T. *Numerical simulation of LCO2 droplet plume in the deep ocean*. Proc. ASME.FEDSM2000-11149, ., 2000. 1–7.

[19] Sato, T. and Sato, K. *Numerical prediction of the dilution process and its biological impacts in CO2 ocean sequestration,* Journal of Marine Science and Technology, 2002. 6(4), 169-180.

[20] Kano, Y., Sato T., Kita J., Hirabayashi S. and Tabeta S. *Model prediction on the rise of pCO2 in uniform flows by leakage of CO2 purposefully stored under the seabed*, Int. J. Greenhouse Gas Contol, 2009. 3. 617-625

[21] Kano, Y., Sato, T., Kita, J., Hirabayashi, S. and Tabeta, S. *Multi-scale modeling of CO2 dispersion leaked from seafloor off the Japanese coast,* Marine Pollution Bulletin, 2010. 60(2), 215-224.

[22] Unesco. *Tenth Report of the Joint Panel on Oceanographic Tables and Standards*. Unesco Technical Papers in Marine Science, 1981. No. 36, 24–29.

[23] M. Ito. *Chemical handbook*, 3rd ed. Tokyo: The Chemical Society of Japan, Maruzen Publishing Company, 1984. 553–558

[24] Someya, S., Bando, S., Song, Y., Chen, B. and Nishio, M. *DeLIF measurement of pH distribution around dissolving CO_2 droplet in high pressure vessel*, International Journal of Heat and Mass Transfer, 2005. 48(12), 2508-2515.

[25] Clift, R., Grace, J. R. and Weber, M. E. *Bubbles, drops and particles*, Academic P. 1978.

[26] Bozzano, G. and Dente, M. *Shape and terminal velocity of single bubble motion: a novel approach*, Computers & Chemical Engineering, 2001. 25(4-6), 571-576.

[27] Zheng, L. and Yapa, P. D. *Modeling gas dissolution in deepwater oil/gas spills*, Journal of Marine Systems, 2002. 31(4), 299-309.

[28] Kulkarni, A.A., Joshi, J.B. *Bubble formation and bubble rise velocity in gas–liquid systems: a review*. Industrial and Engineering Chemistry Research, 2005. 44, 5873–5931

[29] Espinoza, D. N. and Santamarina, J. C., *Water-CO2-mineral systems: Interfacial tension, contact angle, and diffusion—Implications to CO2 geological storage*, Water Resour. Res. 2010, 46(7), W07537.

[30] Coriolis, *Coriolis : In situ data for operational oceanography*. [online] Available at: <http:// http://www.coriolis.eu.org> [Accessed 16 February 2012].

[31] Delhez, E.J.M and Martin, G. Preliminary results of 3D baroclinic numerical models of the mesoscale and macroscale circulation on the North-Western European Continental Shelf, Journal of Marine Systems, 1992. 3, 423–440.

[32] Klusman, R.W. *Rate measurements and detection of gas microseepage to the atmosphere from an enhanced oil recovery/sequestration project, Rangely, Colorado, USA.* Applied Geochemistry , 2003, 18, 1825–1838.